AD-A129 607 DEVELOPMENT OF A SWEEP-FREQUENCY ELECTROMAGNETIC EXPLORATION METHOD FOR T..(U) NORTH CAROLINA STATE UNIV RALEIGH DEPT OF MARINE EARTH AND AT.. I J WON MAY 83 1/1

UNCLASSIFIED ARO-16265.2-GS DAAG29-79-C-0057 F/G 8/7 NL

END
DATE
FILMED
7 83

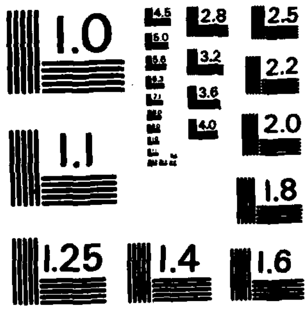

MICROCOPY RESOLUTION TEST CHART
NATIONAL BUREAU OF STANDARDS-1963-A

Unclassified

SECURITY CLASSIFICATION OF THIS PAGE (When Data Entered)

REPORT DOCUMENTATION PAGE		READ INSTRUCTIONS BEFORE COMPLETING FORM
1. REPORT NUMBER 16265.2-GS	2. GOVT ACCESSION NO. AD-A129607	3. RECIPIENT'S CATALOG NUMBER
4. TITLE (and Subtitle) Development of a Sweep-Frequency Electromagnetic Exploration Method for Three-Dimensional Terrain Analysis		5. TYPE OF REPORT & PERIOD COVERED Final: 15 Mar 79 - 14 Mar 83
		6. PERFORMING ORG. REPORT NUMBER
7. AUTHOR(s) I. J. Won		8. CONTRACT OR GRANT NUMBER(s) DAAG29 79 C 0057
9. PERFORMING ORGANIZATION NAME AND ADDRESS North Carolina State University Raleigh, NC 27650		10. PROGRAM ELEMENT, PROJECT, TASK AREA & WORK UNIT NUMBERS
11. CONTROLLING OFFICE NAME AND ADDRESS U. S. Army Research Office Post Office Box 12211 Research Triangle Park, NC 27709		12. REPORT DATE May 83
		13. NUMBER OF PAGES 14
14. MONITORING AGENCY NAME & ADDRESS(if different from Controlling Office)		15. SECURITY CLASS. (of this report) Unclassified
		15a. DECLASSIFICATION/DOWNGRADING SCHEDULE

16. DISTRIBUTION STATEMENT (of this Report)

Approved for public release; distribution unlimited.

DTIC ELECTE JUN 22 1983 S A

17. DISTRIBUTION STATEMENT (of the abstract entered in Block 20, if different from Report)

18. SUPPLEMENTARY NOTES

The view, opinions, and/or findings contained in this report are those of the author(s) and should not be construed as an official Department of the Army position, policy, or decision, unless so designated by other documentation

19. KEY WORDS (Continue on reverse side if necessary and identify by block number)

terrain analysis
geology
electromagnetic systems

20. ABSTRACT (Continue on reverse side if necessary and identify by block number)

During the period of the present research contract: ~~(DAAG29 79 C 0057) we have accomplished the following task stipulated in the contract.~~

(1) We have completed the design and construction of a prototype sweep-frequency electromagnetic exploration system;

(2) We have tested extensively a prototype swept-frequency electromagnetic system on various geological environments and demonstrated the system capability to delineate subsurface geological structures of the earth; (cont)

DD FORM 1 JAN 73 1473 EDITION OF 1 NOV 65 IS OBSOLETE

UNCLASSIFIED

SECURITY CLASSIFICATION OF THIS PAGE (When Data Entered)

83 06 21 017

ADA129607

DTIC FILE COPY

(12)

Abstract (cont.)

(3) We have initiated several theoretical approaches suitable for the interpretation of the spectral profiles generated by the swept-frequency system which are to be correlated with geological structures.

Accession For
NTIS GRA&I
DTIC TAB
Unannounced
Justification
By
Distribution/
Availability Codes
Dist | Avail and/or Special
A

DTIC COPY INSPECTED

Final Report to

Geoscience Division
U.S. Army Research Office
Research Triangle Park, NC 27709

on

Development of a Sweep-frequency Electromagnetic Exploration Method for Three-dimensional Terrain Analysis

(ARO Contract No. DAAG29-79-C-0057)

Submitted by

I.J. Won
Associate Professor of Geophysics
Department of Marine, Earth and Atmospheric Sciences
North Carolina State University
Raleigh, North Carolina 27650

May 1983

Summary

During the period of the present research contract (DAAG-29-C-0057) we have accomplished the following task stipulated in the contract.

(1) We have completed the design and construction of a prototype sweep-frequency electromagnetic exploration system.

(2) We have tested extensively a prototype swept-frequency electromagnetic system on various geological environments and demonstrated the system capability to delineate subsurface geological structures of the earth.

(3) We have initiated several theoretical approaches suitable for the interpretation of the spectral profiles generated by the swept-frequency system which are to be correlated with geological structures.

Introduction

The electromagnetic (EM) systems employing frequencies up to the RF band have long been in use in the mining industry for detecting mineral deposits. The method often referred to as the induction EM method in mining geophysics, involves the propagation of a time-varying low frequency EM field in and over the earth. The available commercial systems are usually designed for a single frequency or a few discrete frequencies, thereby ignoring perhaps the most important aspect of the wave property, namely, the spectral behavior.

Ideally, a geophysical exploration survey not only locates a sought object but also delineates the three-dimensional geologic structure which surrounds the object. The EM method offers a theoretical possibility of rapidly and economically mapping the 3-D subsurface variations. These variations may be due to mineral deposits, groundwater, stratigraphic structures, or any other associated geological conditions having some contrast in electrical properties.

With the advent of several multi-frequency systems during the past decade, the EM frequency-sounding methods have become an important means of investigating the layered geological structure. Their applications have gradually extended to exploration of petroleum, ground water, and geothermal resources as well as determination of permafrost thickness and foundation engineering.

The present research pertains to developing a method of interpreting a continuous spectral profile in order to delineate the underlying geological structure. A spectral profile is a composite of wideband EM response spectra displayed in a frequency-distance space. We assume that the field data are obtained by a loop-loop configuration with a fixed transmitter-receiver separation, a typical frequency sounding setup. This configuration deserves particular attention because it can be housed as a unit on a moving vehicle for continuous operation, a feature essential for speed and economy to cover a large area. Therefore, we shall restrict the subsequent discussion only to the frequency sounding method.

The groundwork for the EM method as an exploration tool for conductive mineral deposits has been well established as documented by Wait (1962), Grant and West (1965), Keller and Frischknect (1966), Ward (1967), Patra and Mallick (1980), and others. Although the method is based on the well-founded classical EM theory, the applications of the theory to realistic geological conditions have been limited to only simple cases.

The layered earth model has been studied theoretically by many authors. Wait (1955, 1958) developed expressions for the mutual coupling ratios of loops over a homogeneous and a two-layered earth. Frischknecht (1967) tabulated the mutual coupling ratios for various loop-loop configurations over a two-layered earth by numerical integration through the Gaussian quadrature method, disregarding the presence of displacement currents. Dey and Ward (1970) and Ryu et al. (1970) gave formal solutions for loops placed on a multi-layered earth with displacement currents having been taken into account. Glenn et al. (1973) applied the generalized linear inversion theory for vertical magnetic dipole sounding data. Anderson (1974) extended the formulation of Wait (1958) and Frischknecht (1967) to a multi-layered earth model and developed a computer program for both the forward calculation of frequency response and the inversion process using the Marquardt non-linear least-squares technique. Lajoie et al. (1975) presented a new method of computing the EM response of a layered earth using the fast Fourier transform. Verma (1980), using a similar formulation of Wait (1958) and Frischknecht (1967), published master tables of the mutual coupling ratios where integrals were computed by the digital linear filter method.

The frequency sounding method is based on the fact that the depth of exploration is governed by the source frequency. The method is particularly suitable, at least in theory, for continuous geological and stratigraphic mapping, since there exist analytic solutions for both forward and inverse problems for horizontally layered earth models. Several field tests of an experimental wideband system have been performed by Ryu et al. (1972), Ward et al. (1974) and Pridmore et al. (1979). Their system had a frequency range on the order of 10 Hz to 100 kHz at 14 manually switchable discrete frequencies to measure tilt-angle and ellipticity of the polarization ellipse. Several other multifrequency systems have been developed: Biewinga (1977) tested a ground vehicle-mounted system with a switch-selectable frequency range between 100 Hz -100 kHz to measure the mutual impedance ratios from a pair of loop receivers; Hohmann et al. (1978) tested a vector EM system which measures magnetic field amplitude and phase at four frequencies, 26 Hz, 77 Hz, 232 Hz, and 695 Hz and presented the data in a frequency-distance space; Siegel and Pitcher (1978) developed their Scintrex Tridem vertical coplanar airborne EM system which measures in-phase and quadrature components at three frequencies, 500 Hz, 2,000 Hz, and 8,000 Hz to map the conductivity of shallow earth. In a different approach Duncan et al. (1980) used a pseudo-random binary sequence noise as a source signal fed into a long-wire bipole transmitter. The received signals, after processing, contain the spectral response of 0.03 Hz to 15 kHz.

The first laboratory sweep-frequency model study was performed by Won (1980). The study employed a logarithmically-sweeping harmonic wave starting at 4 kHz and ending at 4 mHz using a target made of a graphite slab submerged in a conductive solution. The results suggested that certain spectral profiles have visual correlation with the target geometry. Subsequently, a

vehicle-mounted sweep-frequency field system was developed and tested (Won and Clough, 1981; Won, 1982; Won, 1983).

Theoretically, the time-domain EM method can also be used for the depth-sounding by measuring the complete decay curve of a transient field and transforming it into a Fourier spectrum. Practically, since the transient signal decays extremely fast, it would require a receiver having a huge dynamic range, a large number of digitized samples in a fraction of a second and, subsequently, an extensive operation to transform the time-series into the Fourier spectra. Some of these requirements are still technically impractical. For this reason, such a system has never been realized. Although the frequency-domain and the time-domain are theoretically equivalent, the former has many technical and operational advantages. We believe that the frequency-domain EM method can be developed into an efficent and economical spectral profiler, ultimately on a moving vehicle, to be used for a wide variety of geological investigation.

Description of the Prototype Swept-frequency EM System

Figure 1 shows the block diagram of the system. A sweep-signal generator built into a spectrum analyzer produces a sinusoidal sweep whose frequency is logarithmically swept within a predetermined frequency range. The sweep output of the spectrum analyzer is fed into a power amplifier whose output is connected to a transmitter loop. The transmitter loop is mounted on a 1.8 m by 3.0 m wooden frame. The loop is mounted either horizontally or vertically on a small trailer which houses the two power amplifiers and a power generator. The system can be operated from 500 Hz to 100 kHz with a maximum output of 1.2 kW at 500 Hz.

The magnetic field is measured by a small loop of about 30 cm in diameter, mounted on a beam attached to the hood of the truck. The received signal is fed a into a spectrum analyzer for measuring the amplitude spectrum and into a phasemeter for measuring the phase spectrum. The entire measurement cycle, from the activation of the sweep generator to the data recording, is automated by a microcomputer. The measurements can be made either manually at each site or automatically at a preset time-interval for a moving vehicle operation.

At each site, a prescribed number of sweeps is generated. Each sweep consists of a number of stepwise changes in frequency, typically between 50 to 250 steps. The microcomputer generates a linear algebraic series and, through a D/A converter, feeds the stepping voltage into the spectrum analyzer which in turn converts it through a voltage-to-frequency converter into a logarithmically sweeping sinusoidal waveform.

At the end of each step, the received amplitude and phase spectra are digitized and recorded on a temporary storage memory. By waiting until the end of a step, we allow the system to stabilize sufficiently at the new output frequency. As an example, for a sweep duration of two seconds employing 100 steps, each step lasts 20 milliseconds. The signals are sampled and recorded during the last 0.07 milliseconds.

Each digitized spectrum is arithmetically added to the previous spectrum to enhance the signal-to-noise ratio. The final stacked spectrum is then stored on a disk. Since the resolution of the A/D converter is 12 bits, a stack of, say, ten gives a maximum resolution of 0.0024%. In reality, however, the natural and cultural noise, as well as the relative change in the transmitter and receiver loop configuration, may considerably degrade the signal quality.

With the present set-up, we can achieve a minimum sweep duration of about 1.5 seconds. This limit is imposed by the time-constant of the spectrum analyzer. With improved instrumentation, it is believed that the sweep speed can be reduced to one second or less for a possible airborne operation. On the other hand, the lower limit of frequency also dictates the sweep speed: the lower the frequency, the longer the sweep-time required.

The field data can be played back immediately after a profile is completed. First, an average spectrum is computed from the entire profile. The average spectrum thus obtained contains both the overall system response and the mean geological response of the surveyed area. This average spectrum is then subtracted from each original spectrum resulting in an 'anomalous' spectrum. While the removal of the average spectrum does bring out the effects of lateral variation, it has a disadvantage of removing the average properties of the electrical section along the profile.

Figure 2 shows an example of the spectral profile obtained along an existing six-lane highway about 7 miles south of Raleigh, N.C. The section also shows the available surface geological data as well as identifiable cultural features. The profile, about 3,500 feet long, was recorded while the vehicle was moving at about 5 miles per hour employing a horizontal co-planar coils configuration. We stacked a total of five sweeps, each sweep lasting two seconds and having 70 discrete frequency steps. Each gray scale represents a 0.1 db contour interval. The amplitude increases as the shade darkens.

The prominent anomalies at stations 13-18 and 24-27 are well correlated with the outcropping graphite veins as shown on the accompanying section. The anomalies due to man-made objects, such as bridges and culverts, are easily recognizable because their anomalies are narrow and of amplitude high enough to wipe out the entire section. In contrast, the geological objects show spatially distributed anomaly patterns.

Interpretation of Spectral EM Data

In order to interpret a spectral profile displayed in the frequency-distance space, we now turn to the theoretical aspect of a layered earth model. Figure 3 shows theoretical profiles of amplitude and phase for the accompanying geological model, computed from Anderson's program (Anderson, 1974). The computed spectra are approximate in the sense that the layers were assumed to be horizontal below each calculation point. The conductive second layer has a constant thickness of 10 m. At each point the amplitude and phase spectra are computed for 12 frequencies per decade between 100 Hz and 100 kHz. The transmitter and receiver are assumed to be 10 m apart and of a horizontal-

coplaner configuration at an elevation of 2 m above ground.

The amplitude spectrum plotted here is derived as follows: after computing the entire spectra for all stations, we first determined algebraically an average spectrum. This average spectrum was then subtracted from each original spectrum to produce the residual spectral profiles shown in Figure 3. The contour interval is 0.2 db for amplitude and 10 degree for phase. This process removes most of the half space response leaving only relatively anomalous spectral features. The process is identical to one applied to the field data. The theoretical spectral profile suggests that there exist certain visual relationships between the geological model and the resultant spectral profiles. Obviously, the nature of the correlation is complicated and needs further study.

While the above discussion pertains only to the spectral profiles of the magnetic field, further improvements, in terms of the correlation between the subsurface geometry and the spectral profile, may be achieved from the impedance spectra, a ratio of orthogonal magnetic and electric fields. We have not yet tested this possibility theoretically for a loop-loop configuration. However, we present a much simpler case of a plane-wave source over a horizontally layered earth, and show the correlation between the subsurface geometry and the impedance spectral section.

Over a layered earth, the apparent surface impedance is related to the resistivity of each layer through the ratio of the horizontal electric field and the vertical magnetic field (e.g., Jackson et. al., 1962; Kraichmann, 1970). Figure 4 shows the theoretical impedance spectra in the frequency range of 100 Hz - 100 kHz for a three-layered earth. The computation is based on the formula given by Kraichmann (1970). The geometry is intended specifically to model typical ground water environments. At each point on the surface, the layering is assumed to be horizontal for the computation. Dark shades represent high apparent resistivity regions.

The heavy line in the profile is added to denote the frequency at which the amplitude of the incident wave decreases to 1/e (~37%) through the first layer. For a given first layer thickness, this frequency corresponds to that of skin-depth. Figure 4 demonstrates that an impedance spectral profile is, for this case, a considerable improvement over the magnetic spectral profile in terms of the visual correlation with the subsurface resistivity structure.

The section is somewhat similar to the reflection seismic section where the reflected events in a time-distance section have a visual correlation with the reflector geometry. The time-section can be converted into a depth-section if the average velocity up to the horizon is known. In contrast, the impedance section is a function of frequency, which may be converted into depth if the vertical resistivity structure is known. As in the case of the reflection seismic section, the impedance section by itself reveals the relative structure without converting it to a depth section.

Practically, a measured impedance profile may be used to connect one or more sets of drill hole data without laborious interpretation or inversion of the spectra into a depth section. Figure 4 clearly shows this possibility for the case of the plane wave source. To find whether such an prima-facie relation exists under a near-field loop-loop configuration requires further

study. However, laboratory model experiments and limited theoretical analysis by Won (1980) using a sweep-frequency source employing a loop-loop configuration demonstrated that such a relationship may be indeed possible.

Theoretical Considerations

During the past several years we have gained experience in the theoretical study of wideband EM diffraction and in developing the first sweep frequency field system. In this section, we shall discuss some preliminary and fundamental approaches for deriving theoretical wideband spectral responses for several elementary geometries under realistic field conditions. The theoretical results thus obtained will facilitate the understanding and interpretation of wideband data.

As discussed in the previous section, there have been numerous similar studies on various geometries including the layered earth, cylinders, semi-infinite slabs, and spheres. However, most of these solutions are not intended to be used for computing wideband spectral profiles either because of limited bandwidth due to neglecting the displacement current (which may become significant at the high frequency range), or because of numerical impracticality of repetitively computing complex mathematical expressions for several decades of frequencies. The integral representation of EM diffraction problems developed by Won and Kuo (1975a and 1975b) has several advantages for the spectral study: the representation is equally applicable to a wide variety of realistic multi-regional geometries, can accept any variations of electrical conductivity, permittivity, and magnetic permeability, and is not limited in bandwidth since it does not neglect the displacement current. We shall briefly discuss the essential aspect of the method in the following.

Any arbitrary three-dimensional EM diffraction involving two or more different regions (e.g., air, host rock, and a target body) in the presence of an arbitrarily distributed harmonic EM source can be described by a set of six coupled integral equations. These equations can be derived directly from Maxwell's equations without imposing any approximation. Each region is assumed to have different parameters: electric conductivity, permittivity, and magnetic permeability.

The unknowns in these integral equations are the equivalent electric and magnetic surface current densities $\bar{K}$ and $\bar{K}^*$, and the equivalent electric and magnetic surface charge densities η and η^*, induced on each scattering surface. Once these unknowns are determined, the field is described completely everywhere. Since both $\bar{K}$ and $\bar{K}^*$, being vectors tangential to a scattering surface, have two scalar components each, the total unknowns are, thus, six scalars. For a three-region problem having two boundary surfaces, S_α and S_β, we denote the equivalent surface current and charge densities induced on the surfaces S_α and S_β by, respectively, $\mathcal{K}_\alpha$ and $\mathcal{K}_\beta$. By enforcing all six possible boundary conditions on S_α and S_β, we obtain

$$\int_{S_\alpha} [\mathcal{A}]\ [\mathcal{K}_\alpha]\ dS_\alpha + \int_{S_\beta} [\mathcal{C}_{\beta\alpha}]\ [\mathcal{K}_\beta] dS_\beta = [Q^i_\alpha], \text{ and} \tag{1}$$

$$-\int_{S_\alpha} [\mathcal{C}_{\beta\alpha}]\ [\mathcal{K}_\alpha] dS_\alpha + \int_{S_\beta} [\mathcal{B}]\ [\mathcal{K}_\beta] dS_\beta = [Q^i_\beta] \tag{2}$$

Here, $[Q^i_\alpha]$ and $[Q^i_\beta]$ are six component incident primary electric and magnetic fields on S_α and S_β, respectively; the matrices $[\mathcal{A}]$, $[\mathcal{B}]$, and $[C]$'s are of the order of six; $[\mathcal{A}]$ and $[\mathcal{B}]$ are called the geometrical factor matrices of S_α, and S_β, respectively; $[\mathcal{C}_{\alpha\beta}]$ and $[\mathcal{C}_{\beta\alpha}]$ represent the coupling effect between the two adjacent surfaces S_α and S_β, and are referred to as forward and backward interaction matrices. While $[\mathcal{A}]$ and $[\mathcal{B}]$ are mutually independent and solely determined by the shape of their boundary and the electromagnetic property of either side of the boundary, $[\mathcal{C}_{\alpha\beta}]$ and $[\mathcal{C}_{\beta\alpha}]$ are dependent to the mutual geometry of both S_α and S_β, and the property of the medium in between. All matrices are dependent on the frequency of the source, but not on the source location. This fact renders the formulation ideal for repetitively computing a complete profile. It is also obvious that the representations (1) and (2) apply equally well to a borehole survey, as long as one can evaluate the incident field on the boundary surfaces which enclose the source region.

The equivalent surface current and charge densities are not independent, but related to each other through relationships which may be called the conservation of equivalent surface current and charge (Won and Kuo, 1975a):

$$\nabla_s \cdot \overline{K} + \frac{\partial \eta}{\partial t} = -\overline{H} \cdot \nabla_s \times \hat{n}, \quad \text{and} \tag{3a}$$

$$\nabla_s \cdot \overline{K^*} + \frac{\partial \eta^*}{\partial t} = -\overline{E} \cdot \nabla_s \times \hat{n}\ . \tag{3b}$$

where $\overline{E}$ and $\overline{H}$ are the electric and magnetic fields evaluated on S; $\hat{n}$ is a unit normal vector on S; ∇_s denotes a two-dimensional gradient operator on S. If a scattering surface is smooth in the sense that the radii of surface curvature are much larger than the source wavelength, then $\nabla_s \times \hat{n} = 0$ and equations (3a) and (3b) reduce to the familiar continuity equations. In this case, we can eliminate η and η^* in terms of $\overline{K}$ and $\overline{K}^*$, reducing (1) and (2) to two sets of four coupled integral equations. For a two-dimensional diffraction problem, both (1) and (2) decouple, respectively, into two sets of three coupled integral equations: physically, one corresponds to an electric line source problem, and the other to a magnetic line source problem. If the two-dimensional diffraction involves only smooth surfaces, the formulation is reduced again to only two coupled integral equations.

Analytic solutions of equations (1) and (2) may be possible if both S_α and S_β can be traced by separable coordinate surfaces. The analytic approach using the present represe tation is described by Won and Kuo (1975b) in treating a fin ely cond tive circular cylinder embedded in a conductive

whole space in the presence of a line or a dipole source. It has been proved analytically that, for the simplest case of a homogeneous half-space with an electric line source, equations (1) and (2) degenerate to only one integral expression identical to the one derived by Wait (1962, p. 25). For more general problems, we may be forced to solve equations (1) and (2) numerically.

A popular technique for numerically solving integral equations is the method of moment as described by Harrington (1968). The method, in essence, is an approximate linearization process which assumes a certain functional form of the unknown in a whole range or in each subsectional range. Suppose we have N subsections in which the boundary conditions are applied. Then, each integral equation (1) and (2) expands into N simultaneous linear equations. Adopting this procedure, we may rewrite (1) and (2) in pure matrix equation forms:

$$AK_\alpha + C_{\beta\alpha} K_\beta = Q_\alpha, \tag{4}$$

$$-C_{\alpha\beta} K_\alpha + BK_\beta = Q_\beta, \tag{5}$$

where now A, B, and C's denote the matrices expanded in the manner described above. Once (4) and (5) are formulated, the subsequent steps are very straightforward. For most cases, the source is above or on the half space S_α, in which case $Q_\beta = 0$. Solving (4) and (5) for K_α, we obtain

$$K_\alpha = [A + C_{\beta\alpha} B^{-1} C_{\alpha\beta}]^{-1} Q_\alpha . \tag{6}$$

In case the source is located between S_α and S_β, such as in borehole measurements, the Q_α in (6) should be replaced with $[Q_\alpha - C_{\beta\alpha} B^{-1} Q_\beta]$, which may be interpreted as the effective incident field on S_α due to the presence of S_β. The size of matrices A, B, and C's is, for a three-dimensional problem, of an order of 6N and, for a two-dimensional problem, of an order of 3N. Specific expressions for the geometrical matrices and the interaction matrices are given by Won and Kuo (1975a). Also, they discuss extension of the theory to problems having more than three regions.

Equations (1) and (2) degenerate considerably for a layered earth because of the vanishing curvature, thereby eliminating the unknown surface charge density functions. The entire representation can be reduced to an analytic expression which may have to be evaluated numerically. We shall be able to obtain the spectral profiles in the range of 10 Hz to 100 kHz for an undulating layered earth similar to the geometry shown in Figures 3 and 4, assuming that at each data point the earth is horizontally layered (a common assumption in the reflection seismic method). The effects of loop spacing and height should be investigated for various models.

Despite the fact that the layered earth model has been studied by many authors, the model has not been used comprehensively in terms of its spectral responses. Other than for a low frequency range mostly using natural sources such as those in MT survey, the EM method measuring continuous spectral

response rarely has been considered as a stratigraphic mapping tool. While the EM method is used mainly for locating isolated conductive orebodies, there is a strong theoretical possibility that the method can be expanded for wide use utilizing the spectral profiles displayed in a frequency-distance space. We expect that these and other spectral solutions will be obtained based on the foregoing theory through our continuing research efforts on the wideband EM method.

Conclusions

A spectral profile in a frequency-distance domain is somewhat analogous to a reflection seismic profile displayed in a time-distance domain. Although the 3-D seismic diffraction theory is far from complete and somewhat more complicated than the EM diffraction theory, the seismic reflection data are often self-evident in terms of the relative geometry of reflecting horizons.

It is premature to say that the conversion of frequency-distance EM data into a conductivity-depth section would be as definite as the conversion of a seismic time section into a seismic depth section; the spectral EM theory must be developed much further to reach that stage. However, the theoretical and experimental data suggest that such a self-evident interpretation does exist in the spectral EM profiles.

It should be noted, however, that the state of the art is far from complete. Needless to say, we need further theoretical development in wide-band frequency resaponse of realistic earth models as well as advances in experimental schemes. With further progress in these aspects we may be able to develop the present method into an effective efficient tool for exploring geological structures and resources.

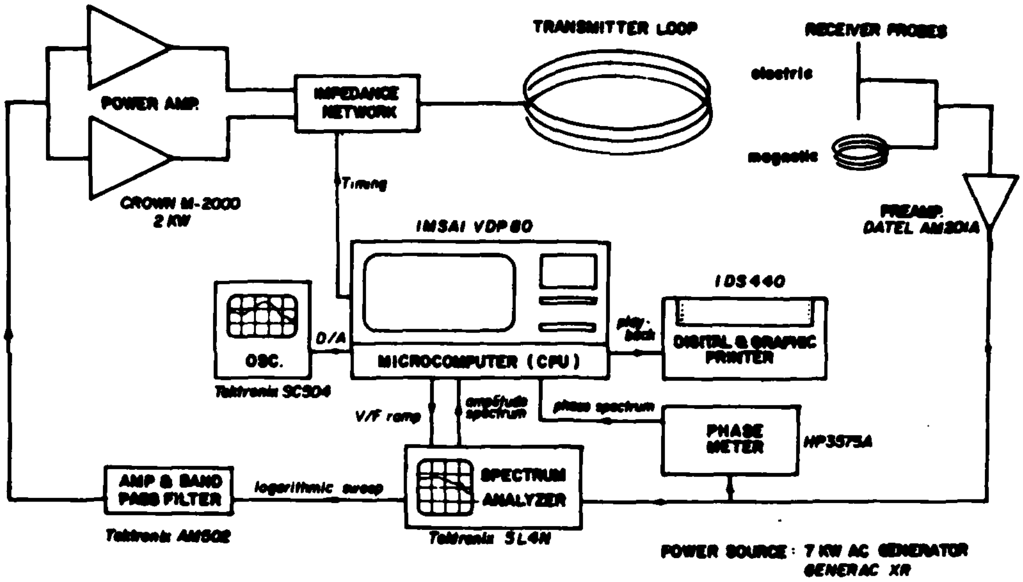

Figure 1. Block diagram of the prototype sweep-frequency electromagnetic system

Figure 2. An amplitude spectral profile section along an existing highway to the south of Raleigh, N.C., with the available geological data

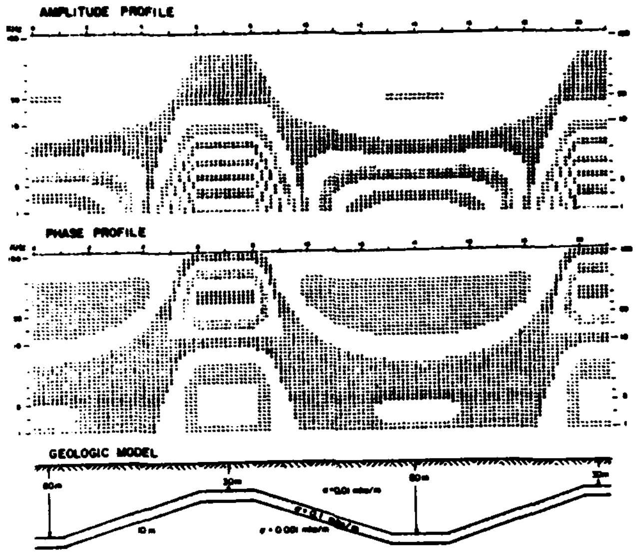

Figure 3. Theoretical amplitude and phase spectra for a three-layer geological model under a horizontal magnetic dipole exitation.

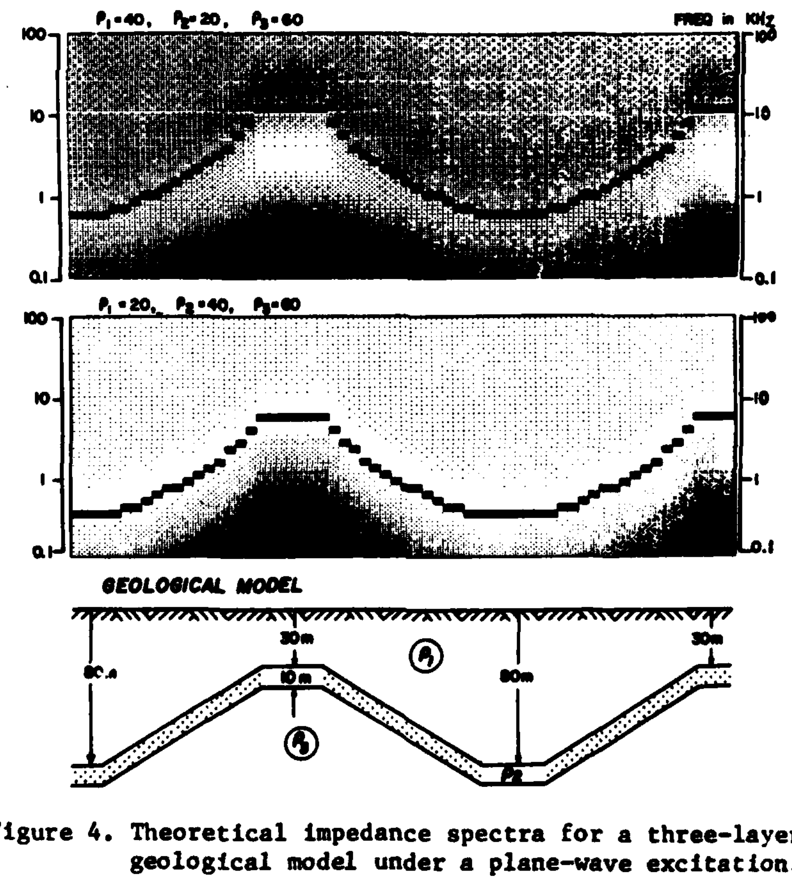

Figure 4. Theoretical impedance spectra for a three-layer geological model under a plane-wave excitation.

References

Anderson, W. L., 1974, Electromagnetic fields about a finite electric wire source: USGS Report GD-74-041, 205 p., NTIS Report PB-238-199.

Biewinga, D. T., 1977, Electromagnetic depth sounding experiments, Geophy. Prosp., 25, 13-28.

Dey, A., and Ward, S. H., 1970, Inductive sounding of a layered earth with a horizontal magnetic dipole, Geophysics, 35, 660-703.

Duncan, P. M., Hwang, A., Edwards, R. N., Bailey, R. C., and Garland, G. D., 1980, The development and application of a wideband electromagnetic sounding system using a pseudo-noise source, Geophysics, 45, 1276-1296.

Frischknecht, F. C., 1967, Fields about an oscillating magnetic dipole over a two-layered earth and applications to ground and airborne electromagnetic surveys: Quarterly of Colorado School of Mines, v. 62, N. 1, 326 p.

Glenn, W. E., Ryu, J., Ward, S. H., Peeples, W. J., and Phillips, R. J.,, 1973, The inversion of magnetic dipole sounding data, Geophysics, v. 38, 1109-1129.

Grant, F. S. and West, G. F., 1965, Interpretation Theory in Applied Geophysics: New York, McGraw-Hill Book Co., Inc., 584 p.

Hohmann, G. W., Vanvoorhis, G. D., and Nelson, P. H., 1978, A vector EM system and its field application, Geophysics, v. 43, 1418-1440.

Jackson, C. M., Wair, J. R. and Walters, L. C., 1962, Numerical results for the surface impedance of a stratified conductor: Nat. Bur. Std. Tech. Note No. 143.

Keller, G. V., and Frischknecht, F. C., 1966, Electrical Methods in Geophysical Prospecting: New York, Pergamon Press, 517 p.

Kraichman, M. B., 1970, Handbook of Electromagnetic Propagation in Conducting Media: HQ, Naval Material Command, U.S. Gov't Printing Office.

Lajoie, J., Alfonso-Roche, J., and West, G. F., 1975, Electromagnetic response of an arbitrary source on a layered earth: A new commputational approach: Geophysics, v. 40, p. 773-789.

Patra, H. P., and Mallick, K., 1980, Time-Varying Geoelectric Soundings, Geosounding Principles 2, Methods in Geochemistry and Geophysics, 14B, Elsevier Scientific Pub. Co., Amsterdam, 419 p.

Pridmore, D. F., Ward, S. H., and Motters, J. W., 1979, Broadband electromagnetic measurements over a massive sulfide prospect, Geophysics, 44, 1677-1699.

Ryu, J., Morrison, H. F., and Ward, S. H., 1972, Electromagnetic depth sounding experiment across Santa Clara Valley: Geophysics, v. 37, p. 351-374.

Siegel, H. O., and Pitcher, D. H., 1978, Mapping earth conductivities using a multifrequency airborne EM system, Geophysics, v. 43, 563-575.

Verma, R. K., 1980, Master Tables for Electromagnetic Depth Sounding Interpretation, IFI/Plenum Data Co., New York, 473 p.

Wait, J. R., 1955, Mutual electromagnetic coupling of loops over a homogeneous ground, Geophysics, v. 20, 630-637.

Wait, J. R., 1958, Induction by an oscillating-magnetic dipole over a two-layered ground, Appl. Sci. Res., v. 7, 73-80.

Wait, J. R., 1962, Electromagnetic Waves in Stratified Media, Pergamon Press, New York, 372 p.

Ward, S. H., 1967, Electromagnetic theory for geophysical applications: Mining Geophysics, v. 2: SEG, Tulsa.

Ward, S. H., Pridmore, D. F., Rijo, L., and Glenn, W. E., 1974, Multi-spectral electromagnetic exploration for sulfides: Geophysics, v. 39, p. 662-682.

Won, I. J., 1980, A wide band electromagnetic exploration method - some theoretical and experimental results: Geophysics, v. 45, p. 928-940.

Won, I. J., 1982, Development of a prototype sweep-frequency electromagnetic exploration system, Geophysics, extended abstract, p. 397-399.

Won, I. J., 1983, A sweep-frequency electromagnetic exploration method, Ch. 2., p. 39-62, in Developments in Geophysical Exploration Methods, Ed., A.A. Fitch, Applied Science Publishers, Ltd, London, 200 p.

Won, I. J. and Clough, J. C., 1981, A sweep-frequency electromagnetic exploration system, Presented at 43rd EAEG Meeting, May, 1981, Venice, Technical Program, p. 42.

Won, I. J., and Kuo, J. T., 1975a, Representation theorems for multiregional electromagnetic diffraction problem, Part I: Theory: Geophysics, v. 40, p. 96-108.

________________, 1975b, Representation theorems for multiregional electromagnetic diffraction problem, Part II, Applications Geophysics, v. 40, p. 109-119.

Final Report to the U.S. Army Research Office
ARO Contract #DAAG29-79-C-0057

APPENDIX A: A reprint from a book entitled "Development in Geophysical Exploration Methods", edited by A.A. Fitch, published by Applied Science Publisher,Ltd, England, 1983.

Chapter 2

A SWEEP-FREQUENCY ELECTROMAGNETIC EXPLORATION METHOD

I. J. Won

North Carolina State University, Raleigh, North Carolina, USA

SUMMARY

A prototype sweep-frequency electromagnetic system has been developed and field-tested. The system, housed in a moving ground vehicle, operates in transit with a loop–loop transmitter and receiver configuration. The transmitter produces logarithmically sweeping harmonic waves between 500 Hz and 100 kHz lasting a few seconds at a maximum output of about 2 kW. Secondary field amplitude and phase spectra are measured, digitised and stacked several times to enhance the signal-to-noise ratio before being transcribed on a disk storage. The entire operational cycle is automated and controlled by an on-board microcomputer. The resultant data are displayed as continuous spectral profiles as a function of distance which may be interpreted as a cross-sectional conductivity structure of the earth in the survey area. Theoretical studies involving several simple models, including a conductive circular cylinder in a conductive half-space, and a horizontally layered earth, suggest that there exist many intuitive correlations between a given geological model and its spectral profile. Laboratory-scale model experiments using a sweep-frequency source also support theoretical predictions of the spectral behaviours.

1. INTRODUCTION

The electromagnetic (EM) exploration system employing a single frequency or a few discrete frequencies up to the RF band has long been in use in the mining industry for detecting mineral deposits which are usually anomalous in electrical conductivity. The method, often referred to as the induction EM method in mining geophysics, involves the propagation of a time-varying low-frequency EM field in and over the earth.

Ideally, a geophysical exploration survey not only locates a sought object but also delineates the three-dimensional (3-D) geological structure which surrounds the object. Thus, it is desirable to develop an EM method which can rapidly and economically map the entire 3-D subsurface variations. These variations may be due to mineral deposits, ground water, stratigraphic or tectonic structures, and any other associated geological conditions having some contrast in electrical properties.

One obvious approach which can provide both deep penetration and high vertical resolution is an EM method employing a wide-band sweep-frequency source. The depth of penetration is mainly determined by the source frequency and ground conductivity. The relationship is shown by the nomogram in Fig. 1. Therefore, applying a sweep-frequency EM field is equivalent to a depth sounding.

The idea of using a wide-band multi-frequency source in the EM method is not new either theoretically or experimentally. To mention a few recently reported field experiments, Ryu *et al.* (1972) used 14 discrete frequencies between 200 Hz and 10 kHz and measured tilt angle, ellipticity and the modulus of wave tilt to explore for ground water in the Santa Clara Valley, California. Similarly, Ward *et al.* (1974, 1977) used 14 discrete frequencies between 10.5 Hz and 86 kHz to explore a sulphide mineral deposit in Cavendish, Ontario.

One of the drawbacks of these systems is that each frequency requires a separate operation. Thus, without introducing fast frequency-multiplexing and power-switching schemes, such a system cannot be used on a moving vehicle. This eliminates its use as a fast (possibly airborne) reconnaissance tool.

There are two main obstacles which have impeded the development of a continuous-frequency EM system: (1) poor theoretical understanding of wide-band induction phenomena, and (2) lack of instrumentation for a high-powered wide-band system with associated field data processing. The theoretical understanding of the wide-band diffraction problem as

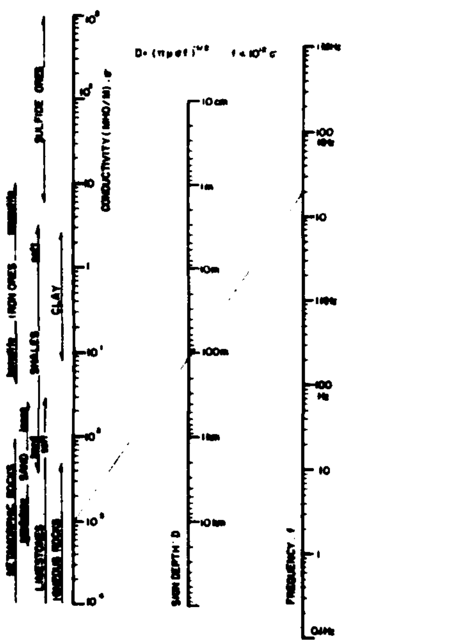

FIG. 1. Relationship between source frequency, ground conductivity and depth of penetration. Magnetic permeability, μ, is assumed to be that of the free space. For example, if the source frequency sweeps from 100 Hz to 100 kHz in a typical igneous rock area, the depth of exploration (skin depth) ranges from about 40 to 1500 m. (From Won, 1980. Courtesy: Society of Exploration Geophysicists.)

applied to EM exploration, although steadily improving, is still primitive except for a few simple geometries. The available theories often become intractable, particularly when all media involved must be considered finitely conductive. On the other hand, the instrumentation difficulties now appear to be quite surmountable with present electronic technology. The large amount of data to be collected in a sweep-frequency EM system is no longer a concern with current high-volume data-logging

techniques, and is rather desirable since a maximum amount of information is gained without appreciable increase in field efforts.

The wide-band diffraction problem essential for developing any continuous-frequency EM system can be attacked by two approaches, namely, solution of Maxwell's equation and model study. Although the method is based on the well-founded classical EM theory (Wait, 1962; Grant and West, 1965; Keller and Frischknecht, 1966; Ward, 1967; and others), the application of the theory to a realistic earth with a finite conductivity contrast between the target and the host medium is extremely difficult, and available solutions are usually band-limited.

A rigorous theoretical spectral study suitable to a sweep-frequency EM system requires a solution to be valid for any frequency with no constraints on the EM parameters, so that the solution can be repetitively evaluated to obtain the entire spectrum. The numerical techniques developed most recently by several authors (Hohmann, 1971, 1975; Parry and Ward, 1971; Won and Kuo, 1975; Lajoie *et al.*, 1975) are powerful in the study of the spectral response, although computationally expensive. While the finite-element method for EM diffraction appears to be promising (Coggon, 1971; Rijo *et al.*, 1977), at present the method does not seem appealing for a fully 3-D problem because of the large computer storage, time and resolution required.

2. THEORETICAL EXAMPLES

Won and Kuo (1975) formulated a generalised EM diffraction theory involving more than two media (e.g. air, host rock, target body), each having an arbitrary electrical conductivity, a dielectric permittivity and a magnetic susceptibility. Won (1980) discussed the case of a circular cylinder of an infinite length in a conductive half-space, as reproduced in Fig. 2. The geometry shown in the inset depicts a circular cylinder having a radius of 50 m and a conductivity of 100 mho/m buried in a half-space of a conductivity of 0.01 mho/m. The source is an insulated wire carrying 1 A placed on the ground directly above the cylinder while the scattered fields are measured at an altitude of 50 m. The figure shows the peak spectral responses of various secondary fields computed at seven different frequencies between 10 Hz and 30 kHz for three different depths (20, 60 and 100 m) of the cylinder.

While the residual magnetic field rapidly decreases as frequency increases, the electric field peaks at a particular frequency which evidently depends on the depth of the cylinder. Since the magnetic field is measured using a loop antenna, the induced EMF which is proportional to frequency will also possess similar peaks. The peaks occur at the frequency at which the corresponding skin depth of the half-space is slightly greater than the actual depth of the target. This can be theoretically explained by considering a constructive interference of a dissipative EM plane wave, as discussed in detail by Won (1980).

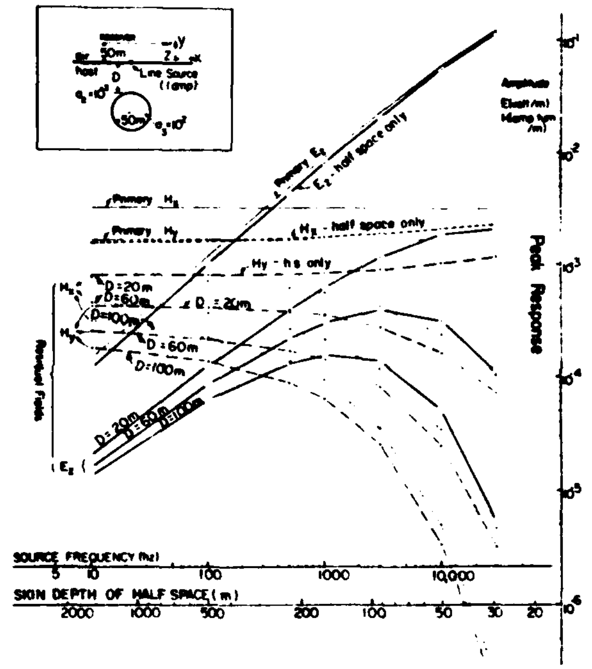

Fig. 2. Peak amplitude response as a function of frequency for a circular cylinder in a half-space at three different depths, 20, 60 and 100 m. Skin depth of the half-space is shown along the frequency axis. (Source: as Fig. 1.)

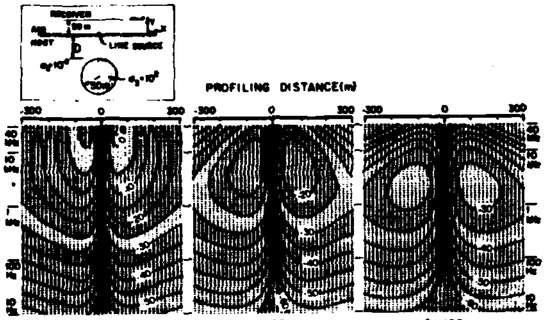

FIG. 3. Theoretically computed amplitude spectral profiles of vertical magnetic field for the situation shown in the inset for various depths, 20, 60 and 100 m. The horizontal axis denotes the profiling distance of the receiver extending 300 m on either side of the circular cylinder located at the centre of the profile. Any single-frequency profile may be obtained by selecting a specific frequency on the vertical axis. The contour interval is 5 dB with an arbitrary reference. (Source: as Fig. 1.)

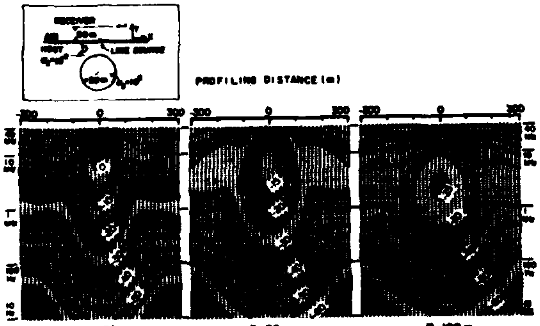

FIG. 4. Theoretically computed amplitude spectral profiles of horizontal magnetic field for the situation shown in the inset for various depths, 20, 60 and 100 m. The horizontal axis denotes the profiling distance of the receiver extending 300 m on either side of the circular cylinder located at the centre of the profile. Any single-frequency profile may be obtained by selecting a specific frequency on the vertical axis. The contour interval is 5 dB with an arbitrary reference. (Source: as Fig. 1.)

As a method of presenting the secondary field data, Won (1980) compiled the profiles for many different frequencies and reduced them to a single spectral cross-section. Figures 3 and 4 show such spectral cross-sections of the vertical and horizontal magnetic fields due to a cylinder at three different depths, 20, 60 and 100 m. Such spectral maps, which are somewhat similar to the geological cross-section derived from the reflection seismic exploration method, may be a very useful means of displaying and investigating a large amount of data at a glance.

3. RESULTS FROM SCALED MODEL EXPERIMENTS

In order to test the theoretical results, Won (1980) experimented with a scaled laboratory sweep-frequency EM system which is shown schematically in Fig. 5. The conductive earth was simulated with saline water, while the target was simulated with a 1.5 cm thick graphite slab 110 × 32 cm.

A carriage on which a transmitter and a receiver were mounted was electrically driven along a fibreglass I-beam. Measurements were made at 2 cm intervals across the target. The transmitter signal consisted of a continuous logarithmic sweep from 4 kHz to 4 MHz for a duration of 30 s. The final amplitude and phase spectra were recorded on an X–Y plotter in real time (and digitised for later machine contouring). The frequency axis of the plot was provided by a triangular ramp voltage which was used to generate the sweep source through a voltage-to-

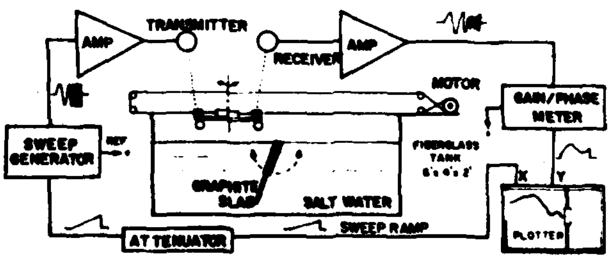

FIG. 5. Block diagram of the EM model system employing a wide-band sweep signal. The field amplitude may be measured in either absolute value or in percentage anomaly compared with the primary field. (Source: as Fig. 1.)

frequency converter. The effect of the tank edge was found to be negligible with the profile distance.

Figures 6 and 7 show the experimentally obtained spectral responses for a vertical graphite slab. The half-space response along with other ambient responses was determined by placing the sensor assembly far from the graphite slab along the profile path. The amplitude and phase spectra at this position were subtracted afterwards. Therefore, these spectra represent only those of residual signals due to the presence of the graphite slab.

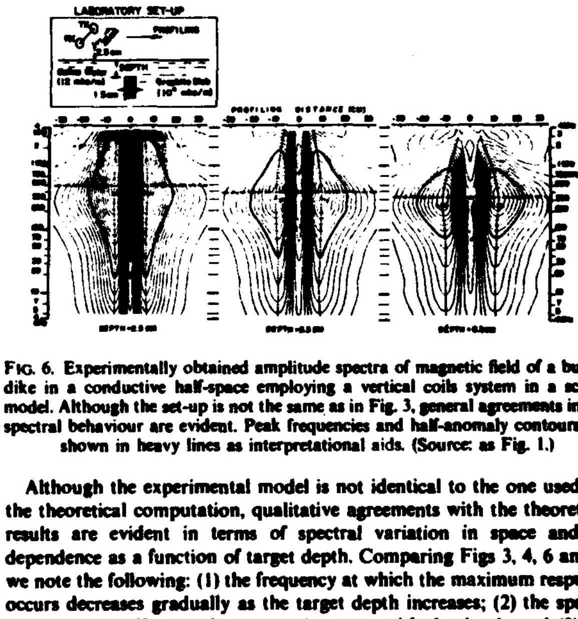

FIG. 6. Experimentally obtained amplitude spectra of magnetic field of a buried dike in a conductive half-space employing a vertical coils system in a scaled model. Although the set-up is not the same as in Fig. 3, general agreements in the spectral behaviour are evident. Peak frequencies and half-anomaly contours are shown in heavy lines as interpretational aids. (Source: as Fig. 1.)

Although the experimental model is not identical to the one used for the theoretical computation, qualitative agreements with the theoretical results are evident in terms of spectral variation in space and its dependence as a function of target depth. Comparing Figs 3, 4, 6 and 7, we note the following: (1) the frequency at which the maximum response occurs decreases gradually as the target depth increases; (2) the spatial width of the half-anomaly contour increases with the depth; and (3) the spectral sections of Figs 4 and 7 for the horizontal magnetic field somewhat resemble the geometrical configuration of the target in the subsurface.

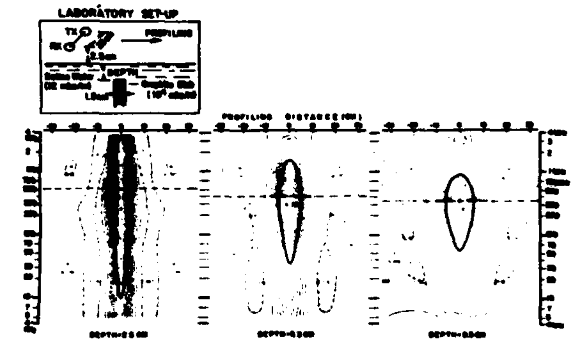

FIG. 7. Experimentally obtained amplitude spectra of magnetic field of a buried dike in a conductive half-space employing a horizontal coils system in a scaled model set-up. (Source: as Fig. 1.)

The spectral characteristics as described above have been qualitatively known and are physically understandable. Rather, the main advantage of such wide-band spectral data is the method of cross-sectionally displaying the entire data in order to provide some intuitive interpretations.

While EM techniques have been in use mostly for minerals exploration, the method in general has a potential application for structural and stratigraphic mapping purposes as well. The latter application, if successful, would have wide usages in many geological problems, particularly if the results show cross-sectional earth structures in a visual format similar to those from the reflection seismic method.

The theoretical EM response of a layered earth has been studied by several authors. Frischknecht (1967) published a comprehensive article on the EM response of a two-layered earth in the presence of an oscillating magnetic dipole. The theory disregards the presence of displacement currents. Anderson (1974) extended it to a multi-layered earth model based upon the theory of Frischknecht, and developed computer programs for both the forward calculation algorithm for frequency response and the inversion algorithm based upon the Marquardt non-linear least-squares technique.

Figure 8 shows the theoretical amplitude and phase profiles for the depicted geological model computed from Anderson's forward-

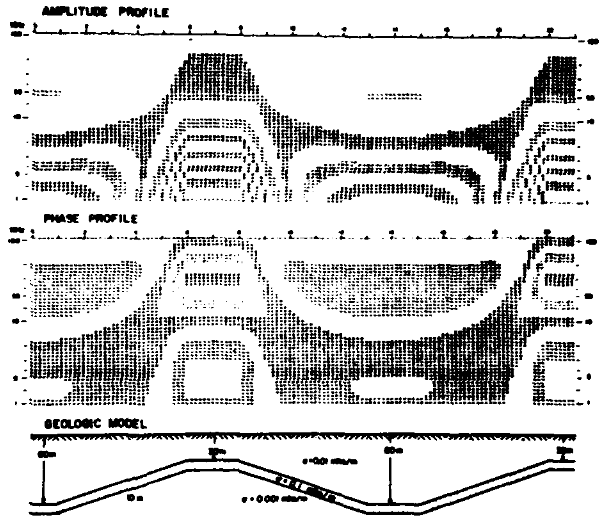

FIG. 8. Theoretical amplitude and phase spectra for the geological model shown, assuming that below each station the earth is horizontally stratified.

calculation algorithm. The computed spectra are approximate in the sense that they are calculated based upon the assumption that the layers were horizontally stratified below each calculation point. The conductive second layer has a constant thickness of 10 m. At each point the amplitude and phase spectra are computed for 12 frequencies for each decade between 1 kHz and 100 kHz. The transmitter and receiver are assumed to be 10 m apart and of horizontal coplanar configuration at an elevation of 2 m above ground.

The amplitude spectrum plotted here is derived as follows: after computing the entire spectra for all stations, we first determined an average spectrum by algebraically averaging the entire spectra; this average spectrum was then subtracted from each original spectrum to produce the 'residual' spectral profiles which are shown in this figure. This process removes most of the half-space response, leaving only

'relatively' anomalous spectral features. (This process will be discussed again later when we encounter the field data.) These theoretical spectral profiles suggest that there exist intuitive relationships between the geological model and the resultant frequency–distance section, somewhat analogous to that of the reflection seismic method. Obviously, the nature of the correlation is complicated and needs further development.

One of the obvious advantages of the spectral profiling technique is to be able to classify any significant anomalies in terms of their subsurface distributions. Physically, an anomaly caused by a large and deep structure will be a broad feature in space and will appear towards the lower end of the spectrum, while an anomaly caused by a small and shallow structure will be a narrow feature in space and will appear towards the higher end of the spectrum. Transition of the spectral peaks as a function of the profile distance can enhance the subsurface features, discriminating against the effects of lateral variations.

4. A PROTOTYPE FIELD SYSTEM

Encouraged by the limited theoretical and laboratory experimental results, we proceeded to build a prototype field system. Figure 9 shows the block diagram of the system. The system may be functionally divided

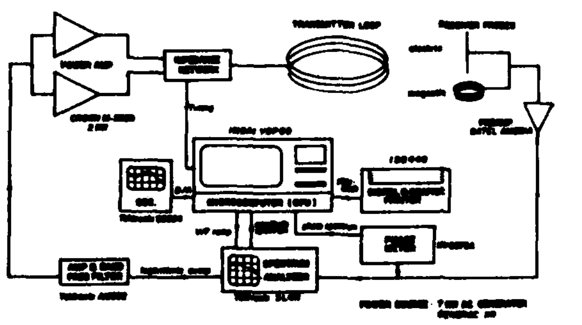

FIG. 9. Block diagram of the sweep-frequency electromagnetic system.

into five subunits: (a) transmitter, (b) receiver, (c) system control, (d) data acquisition and (e) playback. A brief description of each subunit follows.

4.1. Transmitter

A sweep-signal generator built into the spectrum analyser produces a constant-amplitude sweep whose frequency is logarithmically swept within a predetermined frequency range. The unit is driven externally by a microcomputer which generates a linear voltage ramp. This ramp is used by a voltage-to-frequency converter for generating the sweep and provides the frequency axis during measurements. The sweep output of the spectrum analyser is fed into a power amplifier whose output is connected to a radiating transmitter loop. The loop consists of about 20 turns of seven-strand No. 14 copper wire with a thick (THD) insulation, wound on a 1.8 × 3.0 m aluminium frame. The loop is mounted on a small trailer which houses the two power amplifiers and an electrical power generator. The loop can be positioned either horizontally or vertically. Other than the power amplifiers and the generator, the entire system is housed in a small truck.

The loop carries a total resistance of about 1.1 Ω and a total inductance of about 5.5 mH. Since the output impedance of the main power amplifier is about 4 Ω, the lowest frequency the amplifier can accommodate is about 500 Hz with the present loop. This limit can be lowered if we increase the number of turns. However, an increase in turns will result in a power decrease towards the high-frequency end of the spectrum. Presently, the system can be operated from 500 Hz to 100 kHz with a maximum power of 2 kW at 500 Hz.

4.2. Receiver

The secondary magnetic field is measured by a small loop of about 30 cm in diameter. The loop is mounted on a beam attached to the front hood of the truck. The received signal is fed through a modular wide-band preamplifier into the spectrum analyser for measuring the amplitude spectrum and into the phasemeter for measuring the phase spectrum. The phase is referenced to the transmitter signal waveform.

4.3. System Control

The entire measurement cycle, from the activation of the sweep generator to the data transcription, is controlled by the microprocessor unit. The measurements can be repeated either manually at each measurement site or automatically at a preset time interval for a moving vehicle operation.

4.4 Data Acquisition

Figure 10 shows the timing sequence for the system operation. At each measurement point a prescribed number of sweeps are generated and the ground spectral responses in both amplitude and phase are measured. The resultant data are arithmetically stacked in order to enhance the signal-to-noise ratio. Since the resolution of the A/D converter is 12 bits, a stack of, say, ten gives a resolution of 0.0024%. In reality, however, the natural and cultural noise may degrade the signal quality considerably.

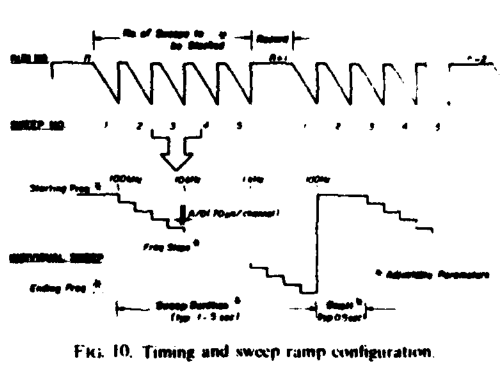

FIG. 10. Timing and sweep ramp configuration.

Each sweep consists of a number of stepwise changes in frequency, typically between 50 and 500 steps. The stepping is accomplished by the microcomputer which generates a linear algebraic series and, through a D/A converter, feeds a stepping ramp voltage into the spectrum analyser. The spectrum analyser, in turn, converts the ramp voltage into a logarithmically sweeping sinusoidal waveform.

At the end of each step the received amplitude and phase spectra are digitised and recorded on a temporary storage memory. By waiting until the end of a step, we allow the system to stabilise sufficiently at the new output frequency. As an example, for a sweep duration of 2 s employing

200 steps, each step lasts 10 ms. The signals are sampled and recorded during the last 0.07 ms. Each digitised spectrum is arithmetically added to the previous spectrum. When all sweeps are completed, the spectrum is then transcribed permanently on a disk storage.

In order to maintain a smooth power consumption cycle, the sweep is made from a high frequency to a low frequency. The output remains at the high-frequency end while idling between sweeps. With the present set-up we can achieve a minimum sweep duration of about 1.5 s. This limit is imposed by the time constant of the spectrum analyser. With an improved spectrum analyser it is believed that the entire sweep speed can be reduced to 1 s or less for an ultimate airborne operation. On the other hand, the lower limit of frequency also dictates the sweep speed: the lower the frequency, the longer the sweep time required.

The several timing parameters shown in Fig. 10 are variable and can be changed, particularly (1) the number of sweeps to be stacked, (2) the number of frequency steps within a sweep, (3) the sweep duration, (4) the starting frequency, (5) the ending frequency and (6) the dwell time between sweeps.

4.5. Playback

The field data can be played back immediately after a profile is completed. First, an average spectrum is computed from the entire profile. The average spectrum thus obtained contains both the overall system response and the mean geological response of the surveyed area. This average spectrum is then subtracted from each original spectrum, resulting in an 'anomalous' spectrum.

5. PRELIMINARY TEST RESULTS

Figure 11 shows a test profile made across two known diabase dikes in Triassic clay in Chatham County, North Carolina. Based upon shallow drill data, both dikes are believed to be almost vertical (~85° dip to the east, i.e. to the right of the profile). Other than these two dikes, the area is composed of various types of soils, mostly clay.

The vertical frequency axis may be converted into a pseudo-depth scale using the skin-depth relationship. If we take a clay conductivity of, say, 0.1 mho/m, the vertical scale would extend to about 90 m.

The contour map is a composite of 32 spectra spaced at intervals of 10 m, and employing a maximum-coupled horizontal coplanar coils

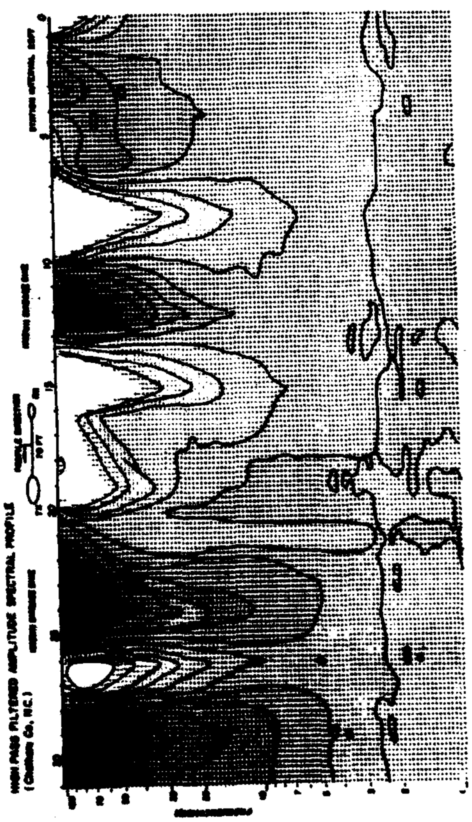

FIG. 11. Amplitude spectral profile over two known diabase dikes in a Triassic basin of North Carolina. From drill data, the dikes are believed to be dipping about 85° to the east (to the right). The dikes are hosted by various clay formations.

configuration. The plotted amplitude scale is in dB with a maximum anomaly of about 12% in the vicinity of the dikes with respect to the primary field. It is evident that the profile contains considerably anomalous spectral features on and around the target diabase dikes.

However, the profile also contains significant anomalies elsewhere. Since the electrical properties of neither the host clay nor the diabase are well known, it is not clear how much contrast in conductivity between them we may expect. Furthermore, clay possesses a wide range of conductivity (0.01 to ~1 mho/m) depending on its water content. Therefore, it is believed that the spectral fluctuations other than those in the vicinity of the dikes may be due to the conductivity variations within the clay formation, affected by water content or other mineralogical variations.

Various filtering procedures may be performed during the playback. Figure 12 shows a spectral profile containing only the shallow anomalies derived from the same data of Fig. 11. By removing all anomalies at the low-frequency end (deepest section), the shallow features are somewhat emphasised.

Figure 13 shows the amplitude spectral profile obtained across a known vein of graphitic schist hosted by metamorphic rocks chiefly composed of schist and gneiss. The graphite in this area appears to be disseminated on the surface. However, nearby outcrops indicate that the vein width at depth may be about 2–3 ft.

Figure 14 shows one unfiltered amplitude profile approximately 3500 ft over a metamorphic region locally overlain by sediments of variable thickness. The known cultural objects as well as available surface geological data are shown on the approximate geological section. The anomalies due to cultural objects such as bridges and culverts are easily recognisable because their high-frequency anomalies are big enough to wipe out the entire spectral section. In contrast, the geological anomalies are laterally and vertically extended showing spatially distributed anomaly patterns. The profile was made while driving at about 10 km/h speed by stacking five sweeps per station, each sweep lasting 2 s and having 70 discrete frequency steps.

The ground response may be affected by the orientation of the profile as well as the heading of the vehicle. In order to evaluate the effect, we obtained two-way profiles along a portion of the same road. Figure 15 shows the southbound profile while Fig. 16 shows the northbound profile. If the system reproduces correctly, the two profiles should be mirror images of each other. This appears to be roughly the case. Since

FIG. 12. The same data as in Fig. 11 except that the low-frequency (deep source) variations are removed, thus enhancing the high-frequency (shallow source) anomalies.

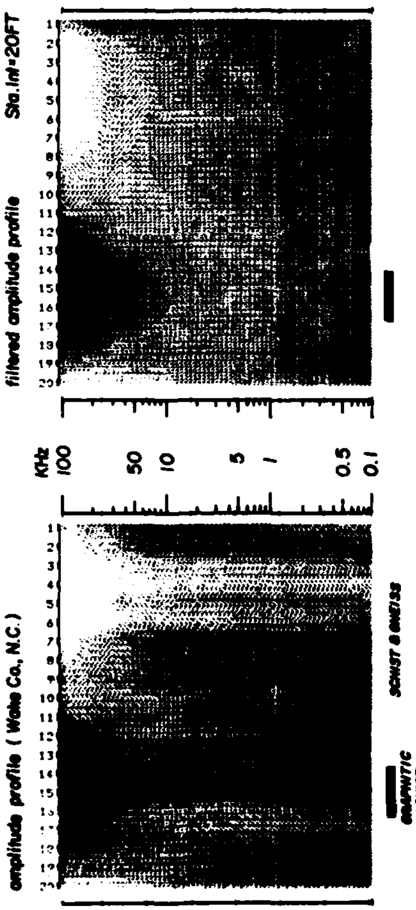

FIG. 13. Amplitude spectral profiles over a known graphite vein.

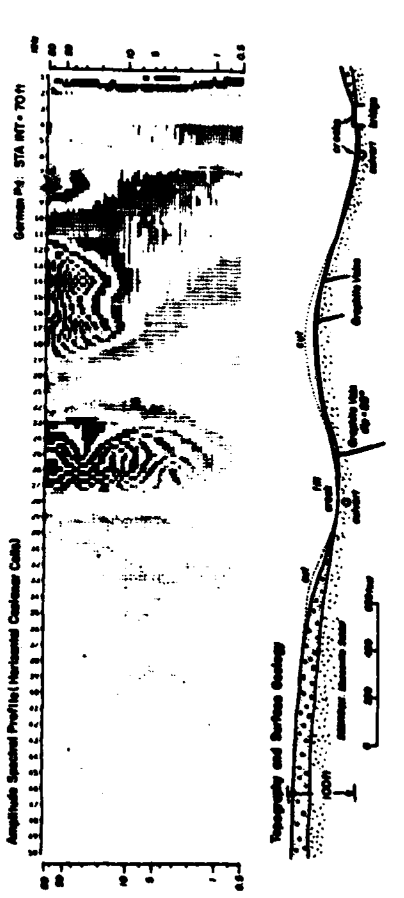

FIG. 14. Amplitude spectral profile from a portion of Gorman Road, south of Raleigh, N.C., along with the available geological data.

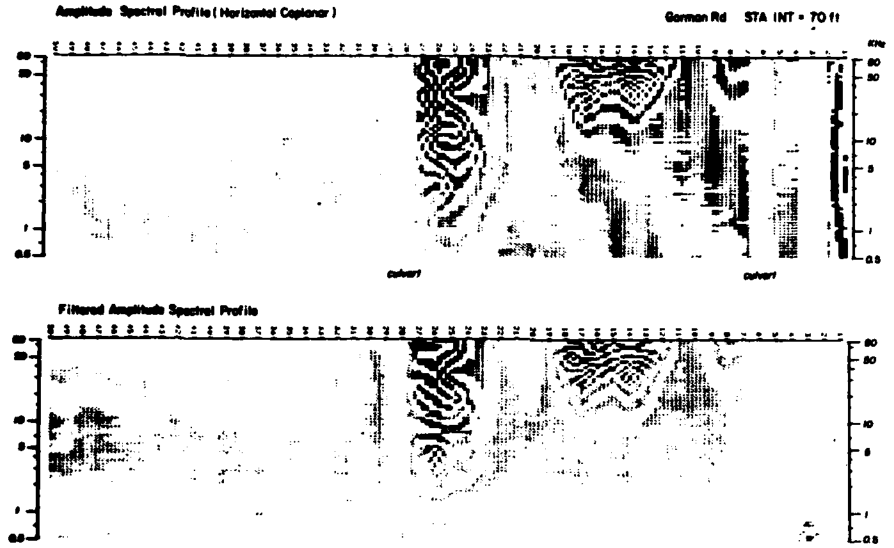

FIG. 15. An [illegible] section from a portion of Gorman Road, south of Raleigh, N.C. All known cultural objects are shown [illegible] amplitude anomalies near stations 12–18 and 23–27 coincide with graphitic schist formations.

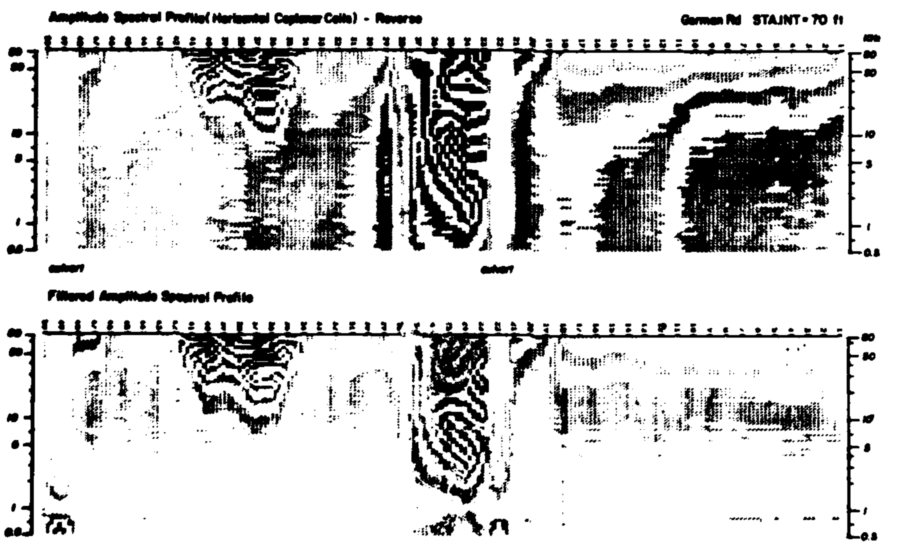

FIG. 16. A reversed profile of the section shown in Fig. 15. This section is made to check reproducibility and effects of vehicle orientation. Since the road is a four-lane highway and the profiles were [illegible] along the shoulder, the two profiles shown in Figs 15 and 16 are about [illegible] apart.

the road is a four-lane highway and the profiles were made along the shoulder, the two profiles are separated by about 100 ft. The two strong anomalies appearing near stations 14 and 25 on the forward profile and near stations 25 and 36 on the reverse profile are believed to be caused by veins of graphitic schist outcropping in the neighbourhood.

Figure 17 show the same area as in Fig. 15 with the corresponding phase spectral profile. The erratic phase spectra between 900–1100 Hz and 65–80 kHz are due to instrumental errors caused by a sudden change in analog output voltage of the phasemeter whenever the phase of the total field changes from -180 to $+180$ or vice versa. By combining both the amplitude and the phase information, one may compute the in-phase or quadrature components as well.

Finally, Fig. 18 shows a profile obtained by a minimum-coupled configuration: horizontal transmitter and vertical receiver coils. The data area is the same as in Fig. 15. The primary field is generally about 40 dB lower than that of the maximum-coupled configuration causing the noisy background. Again, the strong anomalies near stations 22 and 33 are believed to be caused by veins of graphitic schist outcropping in the vicinity. It appears that the system is not sensitive under this configuration.

6. CONCLUSIONS

A spectral profile displayed in a frequency–distance domain is somewhat analogous to a reflection seismic profile displayed in a time–distance domain. Although the 3-D seismic diffraction theory is far from complete and somewhat more complicated than the EM diffraction theory, the seismic reflection data are often self-evident in terms of the relative geometry of reflecting horizons. It is premature to say that the conversion of frequency–distance EM data into a conductivity–depth section would be as definite as the conversion of a seismic time section into a seismic depth section; the spectral EM theory must be developed much further to reach that stage. However, the theoretical and experimental data suggest that such a self-evident interpretation does exist in the spectral EM profiles.

It should be noted, however, that the state of the art is far from complete. Needless to say, we need further theoretical development in wide-band frequency response of realistic earth models as well as advances in experimental schemes. With further progress in these aspects

FIG. 17. The same data as in Fig. 15 with phase spectral profile. Contour interval is 0.4°. The erratic phase spectra between 900–1100 Hz and 65–80 kHz are due to instrumental error (see text).

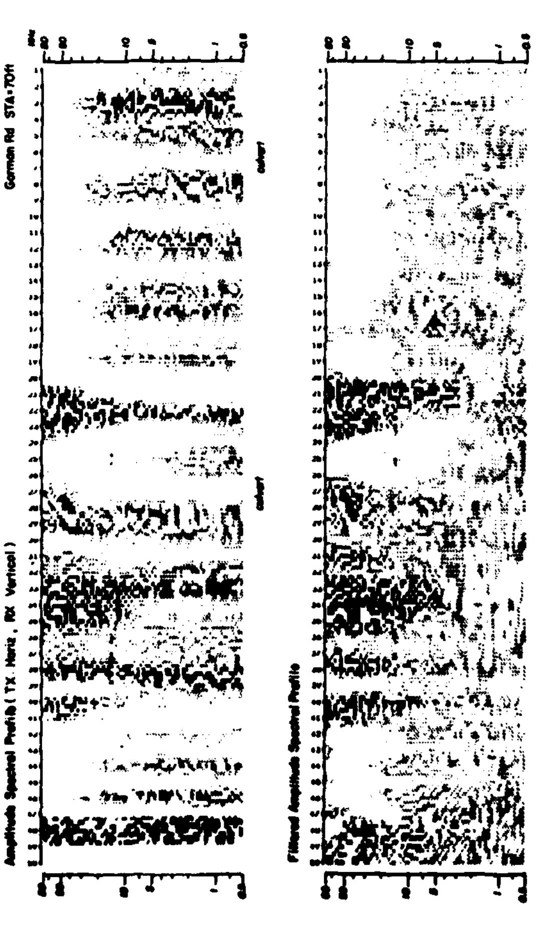

FIG. 18. The same areas as in Fig. 15 measured by a minimum-coupled transmitter and receiver configuration. The primary field amplitude is generally about 40 dB lower than that of the maximum-coupled configuration causing the noisy background.

we may be able to develop the present method into an effective and efficient tool for exploring geological structures and resources.

ACKNOWLEDGEMENTS

The author is grateful to Dr Walter L. Anderson of the US Geological Survey in Denver for making his computer program for computing frequency response of layered earth available to us. This research is supported by the US Army Research Office under contract DAAG29-79-C-0057.

REFERENCES

ANDERSON, W. L. (1974) Electromagnetic fields about a finite electric wire source. US Geol. Serv. Rep. GD-74-041, 205 pp.; NTIS Rep. PB-238-199.

COGGON, J. H. (1971) Electromagnetic and electrical modeling by the finite-element method. *Geophysics* **36**, 132–55.

FRISCHKNECHT, F. C. (1967) Fields about an oscillating magnetic dipole over a two-layered earth and applications to ground and airborne electromagnetic surveys. *Q. Colo. School Mines* **62**(1), 326 pp.

GRANT, F. S. and WEST, G. F. (1965) *Interpretation Theory in Applied Geophysics*, McGraw-Hill, New York, 584 pp.

HOHMANN, G. W. (1971) Electromagnetic scattering by conductors in the earth near a line source of current. *Geophysics* **36**, 101–31.

HOHMANN, G. W. (1975) Three-dimensional induced polarization and electromagnetic modeling. *Geophysics* **40**, 309–24.

KELLER, G. V. and FRISCHKNECHT, F. C. (1966) *Electrical Methods in Geophysical Prospecting*, Pergamon Press, New York, 517 pp.

LAJOIE, J., ALFONSO-ROCHE, J. and WEST, G. F. (1975) Electromagnetic response of an arbitrary source on a layered earth: a new computational approach. *Geophysics* **40**, 773–89.

PARRY, J. R. and WARD, S. J. (1971) Electromagnetic scattering from cylinders of arbitrary cross-section in a conductive half-space. *Geophysics* **36**, 57–100.

RIJO, L., WARD, S. H., HOHMANN, G. W. and SILL, W. K. (1977) On interpretation of broad-band electromagnetic data. Presented at the 47th Annual International Meeting of the Society of Exploration Geophysicists, Calgary, 20 Oct. 1977.

RYU, J., MORRISON, H. F. and WARD, S. H. (1972) Electromagnetic depth sounding experiment across Santa Clara Valley. *Geophysics* **37**, 351–74.

WAIT, J. R. (1962) *Electromagnetic Waves in Stratified Media*, Pergamon Press, New York, 372 pp.

WARD, S. H. (1967) Electromagnetic theory for geophysical applications. In *Mining Geophysics*, Vol. 2, Society of Exploration Geophysicists, Tulsa.

WARD, S. H., PRIDMORE, D. F., RIJO, L. and GLENN, W. E. (1974) Multispectral electromagnetic exploration for sulphides. *Geophysics* **39**, 662–82.
WARD, S. H., PRIDMORE, D. F. and RIJO, L. (1977) *NSF Workshop in Mining Geophysics*, University of Utah, 309 pp.
WON, I. J. (1980) A wide-band electromagnetic exploration method: some theoretical and experimental results. *Geophysics* **45**, 928–40.
WON, I. J. and KUO, J. T. (1975) Representation theorems for multiregional electromagnetic diffraction problem. Part I: Theory. *Geophysics* **40**, 96–108. Part II: Applications. Ibid. **40**, 109–19.

Appendix B: Final Report on ARO#DAAG29-79-C-0057

B-1. Publications resulted from the project

1. A wideband electromagnetic exploration method - Some theoretical and experimental results, I.J. Won, 1980, Geophysics, Vol. 45., p. 928-940.

2. A sweep-frequency electromagnetic exploration system, I.J. Won and J.W. Clough, 1981, European Association of Exploration Geophysicists, Technical Program p. 42, presented at 43rd EAEG Meeting in Venice.

3. Development of a prototype sweep-frequency electromagnetic exploration system, I.J. Won, 1982, Geophysics Extended Abstract, p. 397-399, presented at 52nd SEG Meeting in Dallas.

4. A sweep-frequency electromagnetic exploration method, I.J. Won, 1983, in Chapter 2, Developments in Geophysical Exploration Methods, Edited by A.A. Fitch, Applied Science Publishers, Ltd. England, p. 39-64.

B-2. List of Participating Scientific Personnel

Senior Investigators

I.J. Won   Associate Professor of Geophysics (1979-1982)
J.W. Clough   Assistant Professor of Geophysics (1980-1981)

Graduate Students

Bradley Smith (1980-1982) M.S. Degree 1982
K.H. Son (1981-1982) Ph.D. Candidate
Douglas Washburn (1979-1981)
Joel McDade (1982) M.S. Candidate
Robert Payne (1982) M.S. Candidate

ATE

LME